Subcellular localization and dynamics of a digalactolipid-like epitope in *Toxoplasma gondii*

Cyrille Botté,*,† Nadia Saïdani,*,§ Ricardo Mondragon,** Mónica Mondragón,** Giorgis Isaac,†† Ernest Mui,§§ Rima McLeod,§§ Jean-François Dubremetz,§ Henri Vial,§ Ruth Welti,†† Marie-France Cesbron-Delauw,† Corinne Mercier,1,† and Eric Maréchal1,*

Unité Mixte de Recherche 5168,* Centre National de la Recherche Scientifique-Commissariat à l'Energie Atomique-Institut National de la Recherche Agronomique-Université Joseph Fourier, Institut de Recherches en Technologies et Sciences pour le Vivant, 38058 Grenoble, France; Unité Mixte de Recherche 5163,† Centre National de la Recherche Scientifique-Université Joseph Fourier, Institut Jean Roget, Campus Santé, 38042 Grenoble, France; Unité Mixte de Recherche 5235,§ Centre National de la Recherche Scientifique-Institut National de la Santé et de la Recherche Médicale-Université Montpellier II, 34095 Montpellier, France; Departamento de Bioquímica,** Centro de Investigación y Estudios Avanzados del Instituto Politécnico Nacional, Avenida Instituto Politécnico Nacional 2508, Col. San Pedro Zacatenco, Distrito Federal, México; Division of Biology,†† Kansas State University, Kansas Lipidomics Research Center, Manhattan, KS 66506-4901; and Department of Ophthalmology and Visual Sciences,§§ Pediatrics (Infectious Diseases), Pathology, and Committees on Genetics, Molecular Medicine, and Immunology, University of Chicago, Chicago, IL 60637

Abstract *Toxoplasma gondii* is a unicellular parasite characterized by unique extracellular and intracellular membrane compartments. The lipid composition of subcellular membranes has not been determined, limiting our understanding of lipid homeostasis, control, and trafficking, a series of processes involved in pathogenesis. In addition to a mitochondrion, *Toxoplasma* contains a plastid called the apicoplast. The occurrence of a plastid raised the question of the presence of chloroplast galactolipids. Using three independent rabbit and rat antibodies against digalactosyldiacylglycerol (DGDG) from plant chloroplasts, we detected a class of *Toxoplasma* lipids harboring a digalactolipid-like epitope (DGLE). Immunolabeling characterization supports the notion that the DGLE polar head is similar to that of DGDG. Mass spectrometry analyses indicated that dihexosyl lipids having various hydrophobic moieties (ceramide, diacylglycerol, and acylalkylglycerol) might react with anti-DGDG, but we cannot exclude the possibility that more complex dihexosyl-terminated lipids might also be immunolabeled. DGLE localization was analyzed by immunofluorescence and immunoelectron microscopy and confirmed by subcellular fractionation. No immunolabeling of the apicoplast could be observed. DGLE was scattered in pellicle membrane domains in extracellular tachyzoites and was relocalized to the anterior tip of the cell upon invasion in an actin-dependent manner, providing insights on a possible role in pathogenetic processes.▮ DGLE was detected in other Apicomplexa (i.e., *Neospora*, *Plasmodium*, *Babesia*, and *Cryptosporidium*).—Botté, C., N. Saïdani, R. Mondragon, M. Mondragón, G. Isaac, E. Mui, R. McLeod, J-F. Dubremetz, H. Vial, R. Welti, M-F. Cesbron-Delauw,

C. Mercier, and E. Maréchal. **Subcellular localization and dynamics of a digalactolipid-like epitope in *Toxoplasma gondii*. *J. Lipid Res.* 2008. 49: 746–762.**

Toxoplasma gondii is the unicellular causative agent of toxoplasmosis and one of the parasites of the large Apicomplexa phylum, which includes numerous obligate parasites of both human and veterinary importance (e.g., *Plasmodium, Cryptosporidium, Neospora,* etc.). Like all Apicomplexa, *Toxoplasma* is characterized by unique extracellular and intracellular membrane compartmentalization. *Toxoplasma* resides within the host cell inside a nonfusogenic parasitophorous vacuole (1–5). Its plasma membrane is lined by an inner membrane complex formed by two closely apposed membranes. Inside *Toxoplasma* cells, the endomembrane system (endoplasmic reticulum, nuclear envelope, Golgi network, and plasma membrane) is interconnected with specific apical secretory compartments (i.e., micronemes, rhoptries, and dense granules). These three compartments are sequentially involved in the recognition of and attachment to the host cell (6) and the formation and maturation of the parasitophorous vacuole (4, 7). In addition to a mitochondrion, the envelope of

---

[1] To whom correspondence should be addressed.
e-mail: corinne.mercier@ujf-grenoble.fr (C.M.);
eric.marechal@cea.fr (E.M.)

which has membranes that are disconnected from the endomembrane system, a second semiautonomous organelle has been described in *Toxoplasma* (i.e., a non-photosynthetic plastid called the apicoplast) (8–10). The apicoplast is surrounded by four membranes and was acquired by a secondary endosymbiosis of a red alga (8–11). The outermost membranes of the apicoplast are thought to be reminiscent of the alga plasma membrane and the endosymbiotic phagosome, consistent with their connection with the trafficking vesicular system (12). The two innermost membranes are believed to derive from the envelope membranes of the ancestral algal chloroplast, although no evidence could be provided that the constituents of these membranes were similar to those of the plant chloroplast envelope. Global analysis of the major lipid classes of *Toxoplasma* was achieved recently using mass spectrometry lipidomic profiling (13). The lipid composition of each membrane compartment has not been determined yet, limiting our understanding of the mechanisms for the homeostasis, control, and subcellular trafficking of membrane lipids in *Toxoplasma*, a series of processes that are critical to understanding pathogenesis.

Intense remodeling of membrane compartments is observed during the *Toxoplasma* life cycle. The biogenesis of the parasitophorous vacuole and cell division require large amounts of polar lipids. Data on membrane lipid synthesis are fragmentary, but they highlight the fact that *Toxoplasma* is an auxotroph for sterols (14) and that the production of acyl lipids relies on orchestrated de novo synthesis and the diversion of precursors from the host cell. Three major and possibly redundant fatty acid synthetic machineries can operate for de novo synthesis: an apicoplast fatty acid synthase of type II (FAS II) (10, 15–21), a cytosolic fatty acid synthase of type I (FAS I) (16), and cytosolic fatty acyl elongases (FAEs) (22, 23). Based on metabolic labeling experiments, Bisanz et al. (24) showed that in free stages, de novo fatty acid synthesis was a source for the acyl moiety of *Toxoplasma* glycerolipids. Because acyl-lipid labeling is abolished by haloxyfop [an inhibitor of plastid acetyl-CoA carboxylases (16)], Bisanz et al. (24) concluded that an active FAS II was essential for the bulk of the acyl-lipid synthesis. Combining conditional mutant analyses and metabolic labeling, Mazumdar et al. (23) showed that FAS II was indeed critical for the biogenesis of the apicoplast itself, and subsequently for the parasite survival, but was unlikely to be the source of acyls for the bulk of acyl lipids. Rather, most *Toxoplasma* glycerolipids appear to be produced using acyls generated by FAS I and/or FAEs, based on thiolactomycin resistance and cerulenin sensitivity (23). Together, these analyses highlight the importance *1*) of *Toxoplasma* FAS and FAEs for bulk acyl-lipid syntheses in free stages and *2*) of FAS II activity for apicoplast biogenesis. Upon invasion, in spite of its autonomous capacity to synthesize acyl lipids, *Toxoplasma* massively scavenges host cell lipid precursors for its membrane biogenesis (24–26).

The presence of the apicoplast in *Toxoplasma* suggested that glycerolipids that are unique to alga and plant plastids might be synthesized by the parasite as well. In particular, monogalactosyldiacylglycerol (MGDG) and digalactosyldi-

acylglycerol (DGDG), which constitute >70% of the membrane lipids from chloroplasts and cyanobacteria (27–30), were sought. The synthesis of three classes of galactolipids has been detected in both *Plasmodium* and *Toxoplasma* cell suspensions after metabolic labeling with radiolabeled UDP-galactose (30). Identification of these low-abundance lipids was attempted by comigration in thin-layer chromatography with standard galactolipids from mammals and plants, hydrolysis of polar heads by galactosidases, and hydrolysis of acyl esters by alkaline treatments. One class exhibited the chromatographic behavior of monogalactosylceramide; the two others coincided with plant MGDG and DGDG (30). After metabolic labeling of acyls with radiolabeled acetate, Bisanz et al. (24) confirmed the synthesis of a galactolipid comigrating with DGDG. *Toxoplasma* lipids exhibiting the analytical and biochemical properties of plant MGDG and DGDG raise the questions of their precise structures, biosynthesis, abundance, localization, and possible roles.

The analysis of minor lipids of *Toxoplasma* is a technical challenge, because of the difficulty of producing sufficient amounts of biological material and the sensitivity of existing techniques. Polyclonal antibodies have been introduced as a new tool to probe the subcellular localization and trafficking of DGDG in plants (31). In this study, we used anti-DGDG antibodies obtained by three independent immunizations of two rabbits and one rat with homogeneously pure chloroplast DGDG for the immunodetection of a class of lipids harboring a digalactolipid-like epitope (DGLE) by immunofluorescence (IF) and immunoelectron microscopy (IEM) throughout the life cycle of *Toxoplasma*. Cell membrane fractionation and mass spectrometry were used to attempt to characterize DGLE structure. The occurrence of DGLE in other apicomplexans was also investigated by immunostaining approaches.

MATERIALS AND METHODS

Lipids

Lipids were either purified from plant material or purchased. The purity of lipids, which is critical for this study, was analyzed carefully by two-dimensional thin-layer chromatography (2D-TLC). MGDG, DGDG, trigalactosyldiacylglycerol (TriGDG), and sulfolipid (SL) were purified from spinach leaf chloroplasts. Briefly, chloroplast lipids were extracted (see below) and a first series of separations by 2D-TLC (see below) allowed the separation of each lipid class; if required, a second series of 2D-TLC allowed the purification to homogeneity of each lipid class. Diacylglycerol (DAG), phosphatidylethanolamine (PE), phosphatidylcholine (PC), phosphatidylglycerol (PG), mono-galactosylcerebroside (MGCB), lactocerebroside (LCB), and sphingomyelin (SM) were purchased from Sigma and checked for purity.

Rabbit and rat anti-DGDG antibodies

Two rabbit polyclonal sera were raised against DGDG (anti-DGDG) by immunization of New Zealand White rabbits (Charles River Laboratories) with 2.5 mg of homogeneously pure DGDG extracted from spinach chloroplast membranes, as described

(30). DGDG used for immunization was purified by 2D-TLC. Briefly, the immunization procedure consisted of a first subcutaneous injection at day 1 (0.35 mg of DGDG in Freund's adjuvant), a second and third series of subcutaneous and intramuscular injections at days 10 and 21 (0.35 mg of DGDG in Freund's adjuvant for both subcutaneous and intramuscular injections), and a fourth and fifth series of injections at days 36 and 50 (0.35 mg of DGDG in Freund's adjuvant for subcutaneous injections and 0.35 mg of DGDG without adjuvant for intramuscular injections) before serum collection at day 57. A rat polyclonal anti-DGDG serum was obtained by immunization of a Lewis rat (Charles River Laboratories) with 2.5 mg of pure DGDG.

Plant material

Photosynthetic *Arabidopsis thaliana* cell suspension was cultured and processed for the IF detection of DGDG in chloroplast membranes as described (31). Chloroplasts and chloroplast envelope membranes from spinach leaves were purified as described (31).

Culture of *Toxoplasma gondii*, *Neospora caninum*, *Cryptosporidium parvum*, and *Plasmodium falciparum*

Toxoplasma gondii tachyzoites [RH; American Type Culture Collection (ATCC) 50174; Prugniaud type (32)] as well as *Neospora caninum* tachyzoites were propagated in human foreskin fibroblasts (HFFs; ATCC CRL-1635). For pellicle enrichment experiments, parasites were amplified in human cervix adenocarcinoma epithelial HeLa cells (ATCC CCL-2). Human cells were grown in DMEM supplemented with 100 U/ml penicillin, 100 µg/ml streptomycin, 2 mM glutamine, and 10% FBS (Gibco). Extracellular parasites were forced through a 26.5 gauge needle to break host cells and were purified by filtration through a 3 µm polycarbonate membrane before use. *Cryptosporidium parvum* oocysts (bovine genotype 2) were purified from feces obtained from calves experimentally infected with an isolate maintained at the Institut National de la Recherche Agronomique Laboratory of Avian Pathology (Nouzilly, France). Feces were layered on a discontinuous sucrose density gradient, and purified oocysts were bleached, counted, and permitted to excyst in a 1.5% taurocholic acid solution in BHK 21 medium (Gibco) for 90 min in a 37°C humidified, 5% CO_2 atmosphere. Parasite suspensions were purified through a 5 µm cellulose acetate filter (Sartorius). Twenty-four hours before infection, confluent human ileocecal adenocarcinoma cells (HCT-8; ATCC CCL 244) maintained in RPMI 1640 medium (Gibco) supplemented with 10% FBS, 100 U/ml penicillin, and 100 µg/ml streptomycin were trypsinized and seeded into four-well tissue culture chambers (Labtek chamber slides; Nunc). A total of 1.25×10^5 parasites were allowed to invade each well containing monolayer at 80–85% confluence for 2 h at 37°C. Parasites that did not enter cells were removed; fresh medium (RPMI 1640 containing 35 mg/l ascorbic acid, 25 mM glucose, 0.1 IU/ml insulin, 15 mM HEPES, 1 mg/ml streptomycin, 100 IU/ml penicillin, and 5% FBS) was added to each well, and parasites were allowed to multiply for 48 h. *Plasmodium falciparum* strain 3D7-infected erythrocytes were maintained at 37°C as described (33). 3D7 *P. falciparum* cultures were enriched in gametocytes as described (34).

Treatment of *T. gondii* with cytoskeleton-specific drugs

Confluent HFF cells grown on coverslips were infected with RH tachyzoites for 24 h and treated with the dinitroaniline herbicide oryzalin (0.5, 1, or 2.5 µM) for 24 h (35), cytochalasin D (1 or 5 µM) for 30 min (36), or butanedione monoxime (20, 30, or 50 µM) for 1 h (36) before IF analysis.

IF

For most experiments, purified extracellular *Toxoplasma* cells were allowed to settle for 10 min on polylysine-coated coverslips. Suspensions of purified tachyzoites were processed for IF, with or without fixation and permeabilization, as mentioned in the text and figures. To visualize the plasma membrane and the inner membrane complex separately, extracellular tachyzoites were incubated in 5% glycerol in PBS for 30 min at 37°C on an orbital wheel, centrifuged at 2,000 rpm for 10 min, and suspended in PBS before being deposited on coverslips. For intracellular observations, HFF cells were grown to confluence on glass coverslips deposited on four-well plates and infected with the different strains of parasites. *Toxoplasma* cells as well as infected cells were fixed for 20 min in 4% paraformaldehyde in PBS, permeabilized with 0.1% Triton X-100 (v/v) in PBS, and blocked using 10% FBS in PBS. For *P. falciparum* 3D7 analyses, infected erythrocytes were fixed in 4% paraformaldehyde in PBS and immobilized on polylysine-coated slides. Fixed parasites were briefly permeabilized in 0.1% Triton X-100 in PBS, and unspecific binding sites were blocked using 10% FBS in PBS. Parasites and infected cells were stained with the following primary antibodies: polyclonal anti-DGDG sera (1:25 or 1:50) (30), polyclonal rat anti-DGDG serum (1:25), polyclonal rabbit anti-IMC1 serum (1:500; a kind gift from C. Beckers, University of North Carolina) (37), polyclonal rabbit anti-GRA6 serum (1:500; a kind gift from L. D. Sibley, Washington University School of Medicine) (38), monoclonal TG19.179 anti-GRA2 antibody (1:500) (39), monoclonal TG054 anti-SAG-1 antibody (1:500) (40), monoclonal T8.4A12.1C3 anti-SRS9 antibody (previously called P36 or BSR4) (41), and polyclonal rat anti-*Cryptosporidium* serum (42). All antibodies were diluted in 1% FBS in PBS and detected using BODIPY or Texas Red-conjugated goat anti-mouse, anti-rabbit, or anti-rat IgG (H+L) antibodies (1:500) (Molecular Probes).

DNA was labeled with 0.5 µg/ml Hoechst (Molecular Probes) for 5–20 min. Coverslips were mounted with the ProLong Antifade Kit (Molecular Probes). Fluorescent images were acquired with an Axiocam MRm (Zeiss) on an inverted Axioplan 2 microscope (Zeiss), and images were acquired with the Axiovision 3.1 software (Zeiss). For *P. falciparum* analyses, parasites containing a single nucleus and lacking the digestive vacuole were considered as ring-stage parasites, those containing a single nucleus and a digestive vacuole were considered as trophozoite-stage parasites, and those containing two nuclei or more and a digestive vacuole were considered as schizont-stage parasites. Anti-DGDG antibodies were incubated at a 1:25 dilution in 10% FBS in PBS during 1 h, and secondary antibodies (either Alexa Fluor 488 or Alexa Fluor 592 goat anti-rabbit) were incubated using a 1:1,000 dilution in 10% FBS in PBS. Nuclei were labeled using Hoechst 33258 by a 5 min incubation at a 1:10,000 dilution in PBS. Detection of DGDG in *Arabidopsis* cells was carried out as described (31) with anti-DGDG at a 1:25 dilution. The fluorescence of chlorophyll (excitation, 543 nm) was collected at 652 nm. Coverslips were mounted with Immu-Mount (Thermo Electron Corp.). Fluorescent images were acquired with a MicroMax 1300 Y/HS charge-coupled device camera (Princeton Instruments) under the control of the Metavue imaging system (Universal Imaging Corp.) on an upright Leica DMRA2 microscope.

IEM

Immunolocalization of DGLE was achieved on extracellular tachyzoites as described (43). Human larynx carcinoma epithelial cells (Hep-2; ATCC-CCL 23) maintained in DMEM (Gibco),

supplemented with 10% FBS (Equitech-Bio) under a 5% CO_2 atmosphere at 37°C, were infected by *Toxoplasma* (infection ratio of 10 parasites to 1 host cell) tachyzoites for 24 h. Infected Hep-2 cells and isolated tachyzoites ($5–7 \times 10^7$/ml) were washed three times with PBS and fixed in 4% paraformaldehyde containing 0.1% glutaraldehyde in serum-free PBS for 1 h at room temperature. Washed parasites were gradually dehydrated in ethanol and embedded in LR White resin (London Resin Co.), which was polymerized overnight, under ultraviolet light, at 4°C. Thin sections were mounted on Formvar-covered nickel grids. Immunolabeling was carried out at room temperature by flotation of the mounted sections on drops of each solution; to minimize nonspecific labeling, grids were incubated with PBS containing 1% skim milk and 0.05% Tween-20 (PBS-MT) for 30 min, and sections were incubated with the anti-DGDG rabbit polyclonal serum (dilution, 1:5 in PBS-MT) for 1 h at room temperature and overnight at 4°C. Grids were thoroughly washed with PBS-T (PBS + 0.05% Tween-20) and then incubated for 2 h at room temperature, with the corresponding secondary antibody (goat anti-rabbit polyclonal antibody) coupled to 10 nm gold particles (Axell) (dilution, 1:40 in PBS-T). Incubation with each antibody solution was performed in a humid chamber with intervening washes. After thorough washing in PBS and distilled water, sections were contrasted with 2% uranyl acetate and a satured solution of lead citrate and then examined with a transmission electron microscope (JEOL 2000 EX). As negative controls, sections were incubated with normal rabbit serum diluted in PBS-MT and then with the secondary antibody coupled to gold particles. As a positive control, sections were incubated with a rabbit polyclonal serum against a whole extract of *Toxoplasma* tachyzoites and then revealed with the secondary antibody coupled to gold particles. Immunolocalization of DGLE in tachyzoite cytoskeletal preparations was carried out as described (44).

Purification and analysis of *Toxoplasma* pellicle

Pellicle (inner membrane complex and plasma membrane) was purified from extracellular *Toxoplasma* parasites by sucrose gradient centrifugation and high-salt glycerol treatment as described (45–47).

Purification and analysis of *Toxoplasma* detergent-resistant membranes

Detergent-resistant membranes (DRMs) were isolated from *Toxoplasma* tachyzoites according to the procedure described previously (48).

Glycerolipid extraction, separation, and quantification

Lipids were extracted from *T. gondii* tachyzoites (2×10^9 cells) and from purified membrane fractions as described (49). Quantification of *Toxoplasma* glycerolipids was performed after methanolysis. Briefly, known amounts of C21:0 fatty acid were added to lipid extracts, then acyl esters were transesterified to the methyl esters and FAs were methylated using 3 ml of 2.5% H_2SO_4 in methanol for 1 h at 100°C. The reaction was stopped by the addition of 3 ml of water and 3 ml of hexane. The hexane phase was analyzed by gas-liquid chromatography (Perkin-Elmer) on a BPX70 (SGE) column. Retention times and peak intensities of fatty acid methyl esters were compared with those of standards. The obtained amount of fatty acids was used to calculate the initial glycerolipid content. Quantified lipids were dried under argon and frozen at −20°C for subsequent analyses.

Sterol extraction and quantification

Sterols (including cholesterol and steryl esters) were extracted and quantified by a resofurin-based fluorometric assay (Calbiochem) according to the manufacturer's instructions.

Acyl-lipid mass spectrometry analysis

Mass spectrometry analyses of *Toxoplasma* pellicle lipid extracts were carried out by injecting 2–20 nmol of total polar lipids per milliliter. Analyses were performed as described previously (13). The sample in chloroform-methanol-300 mM aqueous ammonium acetate (300:665:35) was infused into an Applied Biosystems Q-TRAP with an Advion Triversa microchip electrospray system at 0.11 µl/min (ionization voltage was set to 1.8 kV and gas pressure to 0.1 p.s.i.). Polar lipids from pellicle membranes were determined and quantified based on known amounts of internal standards for each lipid class: phosphatidic acid (PA), LysoPC, PC, ePC [alk(en)yl-acyl phosphocholine], LysoPE, PE, ePE [alk(en)yl-acyl phosphoethanolamine], phosphatidylinositol, phosphatidylserine (PS), ePS [alk(en)yl-acyl phosphoserine], MGDG, DGDG, Cer, EthCer (ceramide phosphoethanolamine), SM (also termed ChoCer or choline ceramide in this paper), and MHexCer and DHexCer. Amounts of lipids with masses coinciding with those of MGDG, DGDG, and PA include weak peaks close to the noise/contamination baseline. To identify potential glycolipids, scans to detect ions producing a neutral loss of 179 (i.e., loss of ammoniated hexose minus water or $[C_6H_{13}O_5N]$) or ions corresponding to neutral loss of 341 (i.e., loss of ammoniated dihexose minus water or $[C_{12}H_{23}O_{10}N]$) were performed. The final profile of acyl lipids, calculated in mol%, was normalized by taking into account the sterol content quantified in the initial sample.

Lipid nitrocellulose dot-blotting and immunolabeling with anti-DGDG sera

MGDG, DGDG, TriGDG, PE, PC, SL, DAG, PG, SM, MGCB, LCB, and total lipid extracts from spinach chloroplast envelope, HFF cells, and *Toxoplasma* were solubilized in butanol and spotted onto a nitrocellulose membrane. Membranes were saturated for 1 h in TBS (10 mM Tris, pH 7.5, and 9 g/l NaCl) complemented with 1% (w/v) nonfat dry milk, incubated with rabbit anti-DGDG serum (1:100), washed, and developed with a goat serum anti-rabbit IgG (H+L) coupled with horseradish peroxidase (1/10,000) (Sigma). For competition assays, anti-DGDG serum [100 µl, 1:100 in 1% (w/v) nonfat dry milk in TBS] was preincubated for 16 h at 4°C with 100 µg of DGDG purified from spinach. Peroxidase activity was revealed in 100 mM Tris-HCl, pH 8.5, 12.5 mM luminol (3-aminophalhydrazine), and 0.2 mM coumaric acid in the presence of H_2O_2. Autoradiography was performed with Hyperfilm ECL (Amersham).

Western blots

Proteins of whole cell extracts or obtained after pellicle fractionation were quantified (50) and separated by SDS-PAGE. After electrophoresis, proteins were stained in isopropanol-acetic acid (3:1, v/v) containing 0.25% (w/v) Coomassie Brilliant Blue (R-250; Sigma) or electrophoretically transferred to nitrocellulose membranes for immunoblotting. Membranes were blocked for 1 h with saturation solution (5% powdered milk, 5% goat serum, 0.05% Tween-20, and 0.05% Triton X-114 in PBS) and incubated for 1 h with primary antibodies: rabbit anti-DGDG serum (1:100), rabbit anti-IMC1 (1:5,000), or monoclonal TG 17.054 anti-SAG1 (1:5,000). After incubation with peroxidase-conjugated goat secondary antibodies (Jackson ImmunoResearch Laboratories), immunolabeled polypeptides were detected using the Supersignal ECL system (Pierce Chemical).

RESULTS

Specific antibodies raised against spinach chloroplast DGDG react with a class of *Toxoplasma* lipids harboring a DGLE

Metabolic labeling experiments with radiolabeled UDP-galactose and acetate have demonstrated the synthesis of a lipid class comigrating with DGDG in *Toxoplasma* (24, 30). In the present study, we attempted to characterize this digalactolipid-like lipid and to provide additional information on its subcellular localization. We made use of rabbit polyclonal antibodies raised against DGDG homogeneously purified from spinach chloroplasts (30, 31). Anti-lipid antibodies are usually more difficult to manipulate than anti-protein antibodies (mainly because of the very different molecular size and hydrophobicity of lipids vs. proteins); they must be used at higher concentrations (dilution 1:100 in nitrocellulose immunostaining assays and 1:25 in IF experiments), require an accurate exposure of the lipid epitope (regions where the lipid is sufficiently concentrated), and cannot be easily purified without an existing method to accurately graft the lipid epitope on a purification matrix. For these reasons, we checked the validity of the experiments presented here with three independent rabbit and rat anti-DGDG sera, controlled the results with those obtained with preimmune serum, and carried out competitive labeling with homogeneously pure DGDG. In this study, the class of *Toxoplasma* lipids harboring a DGLE was named DGLE.

Figure 1 shows the results obtained with one of the rabbit anti-DGDG sera. Purified DGDG (10 μg) and total lipids from the spinach chloroplast envelope (200 μg) spotted on nitrocellulose membranes were used as positive controls for the immunostaining of lipids dot-blotted on nitrocellulose membranes (Fig. 1A). No signal was detected with DAG, phospholipids (PG, PC, PE), SM, monogalactolipids or trigalactolipids (MGDG, TriGDG), sulfoquinovosyldiacylglycerol (SL), MGCBs, or LCBs (Fig. 1A). Other than LCB, MGCB, and SM, all of these lipids share a DAG hydrophobic moiety with DGDG. Therefore, this immunoreactivity profile shows that the rabbit anti-DGDG antibodies react with the digalactolipid polar head. The rabbit polyclonal anti-DGDG antibodies consistently reacted with lipids extracted from the spinach chloroplast envelope and did not react with HFF lipids (200 μg) (Fig. 1A). As a negative control, preimmune serum failed to react with purified DGDG (10 μg), spinach chloroplast envelope lipids (200 μg), or *Toxoplasma* total lipids (200 μg) (Fig. 1B). Consistent with a previous report by Jouhet et al. (31), Fig. 1C shows that the rabbit anti-DGDG serum allows the specific detection of chloroplast membranes of permeabilized *Arabidopsis* cells (DGDG is not extracted from membranes in IF permeabilization treatments). The rabbit anti-DGDG serum did not show any significant cross-reactivity with total protein extracts from *Toxoplasma* or HFF proteins (Fig. 1D).

Figure 1E, F shows the reactivity of the rabbit anti-DGDG serum with *Toxoplasma* lipids. Preincubation of anti-DGDG with purified DGDG abolished the reactivity on purified DGDG and on *Toxoplasma* total lipid extract (Fig. 1E). These results showed that DGDG saturated the anti-DGDG antibodies of the rabbit serum and competed efficiently with the *Toxoplasma* lipids, highlighting the structural similarity between DGDG and DGLE polar heads. Thus, we reasonably supposed that DGDG and DGLE were immunostained with a similar intensity and that a dose-dependent immunoreactivity of the anti-DGDG rabbit serum with increasing amounts of spotted DGDG (Fig. 1F) allowed the relative quantification of DGLE in various *Toxoplasma* and HFF samples. Therefore, the DGLE proportion in *Toxoplasma* total lipids was estimated at ~0.25 mol% (Fig. 1F) and represents a minor lipid class.

A second rabbit and a rat were independently immunized with homogeneously pure DGDG according to the same procedure. The two additional sera obtained after immunization with DGDG reacted similarly with *Toxoplasma* DGLE (data not shown). Collectively, these results support the notion that both rabbit and rat polyclonal antibodies, raised against plant chloroplast DGDG, immunoreact with a class of *Toxoplasma* lipids whose polar heads share structural features with that of DGDG [i.e., terminated by a dihexosyl group structurally close to α-galactosyl (1→6)β-galactose]. Anti-DGDG sera have been used to investigate the subcellular localization of DGLE by IF and IEM experiments. In the experiments described below, results obtained with the first rabbit anti-DGDG serum are presented, except as indicated.

In extracellular *Toxoplasma* parasites, DGLE is localized in membrane domains, at the surface of the plasma membrane, and in the inner membrane complex

To localize DGLE in extracellular parasites, freshly lysed tachyzoites were labeled with the rabbit anti-DGDG serum without any fixation and permeabilization and then observed by epifluorescence. In parallel, parasites were fixed, permeabilized with Triton X-100, and labeled with anti-DGDG (**Fig. 2A**). IF images were captured and signal intensity was enhanced using Axiovision 3.1 software (Zeiss). Preimmune serum did not allow any labeling (Fig. 2A, left). The absence of labeling with anti-IMC1, an antibody raised against an inner membrane protein (IMC-1) (37), was used as a control for plasma membrane integrity (Fig. 2A, right). DGLE was localized with a dotted pattern at the parasite periphery, independently of the permeabilization step (Fig. 2A, center). A series of images focused at the top, medial, and bottom sections of the same parasite showed that the dotted patterns of both non-permeabilized and permeabilized parasites were scattered around the parasitic surface (Fig. 2B) and that no intense labeling could be detected in central compartments of the cell.

To refine the localization of DGLE at the cell periphery, extracellular tachyzoites were treated with 1% glycerol to allow local swelling and osmotic separation of the plasma membrane from the inner membrane complex. Under these conditions, the plasma membrane forms small blebs at the cell surface. Figure 2C shows that the rabbit anti-DGDG serum labeled both the plasma membrane
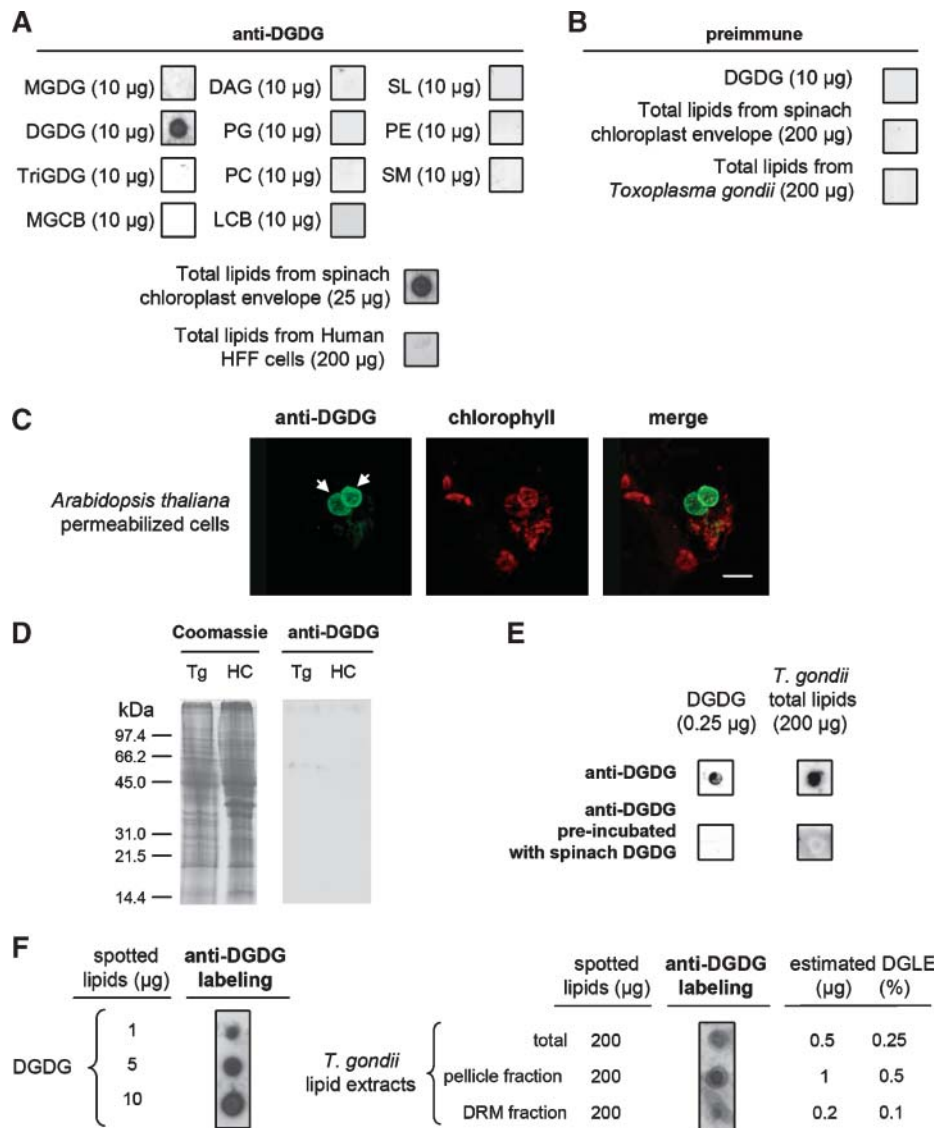
Fig. 1. Immunoblot analyses of lipid standards and *T. gondii* lipid extracts using rabbit anti-digalactosyldiacylglycerol (DGDG) polyclonal antibodies. A: Immunoreactivity of the rabbit anti-DGDG serum toward lipid standards (10 μg) [i.e., diacylglycerol (DAG), DGDG, lactocerebroside (LCB), mono-galactosylcerebroside (MGCB), monogalactosyldiacylglycerol (MGDG), trigalactosyldiacylglycerol (TriGDG), phosphatidylcholine (PC), phosphatidylethanolamine (PE), phosphatidylglycerol (PG), sulfolipid (SL), and sphingomyelin (SM)] and total lipids purified from spinach chloroplast envelope (25 μg) and human foreskin fibroblast (HFF) cells (200 μg). To assess the specificity of the anti-DGDG serum, purified DGDG and total lipids from the spinach chloroplast envelope were used as positive controls. No signal was detected with spotted DAG, phospholipids (PG, PC, and PE), sphingolipid (MGCB, LCB, and SM), or simple glycoglycerolipids such as galactolipids (MGDG and TriGDG) or sulfoquinovosyldiacylglyc-erol (SL). Therefore, this immunostaining profile shows that the anti-DGDG antibodies react with the lipid polar head. B: Immunoreactivity of the preimmune serum against purified DGDG (10 μg), total spinach chloroplast envelope (200 μg), or total *T. gondii* lipids (200 μg). C: Immunofluorescence (IF) immuno-staining of chloroplasts, in permeabilized *Arabidopsis* cells, with the rabbit anti-DGDG serum. D: SDS-PAGE of protein extracts from *Toxoplasma* parasites (Tg) and from HFF host cells (HC) revealed either by Coomassie blue staining (Coomassie) or by immunoblot analysis with the rabbit anti-DGDG serum. E: Immunoreactivity of the rabbit anti-DGDG serum, preincubated for 12 h with purified DGDG, with purified DGDG (0.25 μg) or total *T. gondii* lipids (200 μg) (lower lane) and immunoreactivity of the untreated rab-bit serum anti-DGDG with the same lipids (upper lane). This result highlights the very high structural similarity between the DGDG epitopes and the digalactolipid-like epitope (DGLE). F: Dose-dependent reactivity of the rabbit serum anti-DGDG to increasing quantities of purified spinach DGDG (1, 5, or 10 μg) spotted on a nitrocellulose membrane. Supposing that DGDG and DGLE were immunostained with a similar intensity, the dose-dependent immunoreactivity of the anti-DGDG rabbit serum allowed a relative quan-tification of DGLE in various *Toxoplasma* samples. Total lipid extracts from *T. gondii* (200 μg) as well as pellicle (200 μg) and raft (200 μg) lipid extracts were spotted onto nitrocellulose membranes and probed with the rabbit anti-DGDG serum. DRM, detergent-resistant membrane.
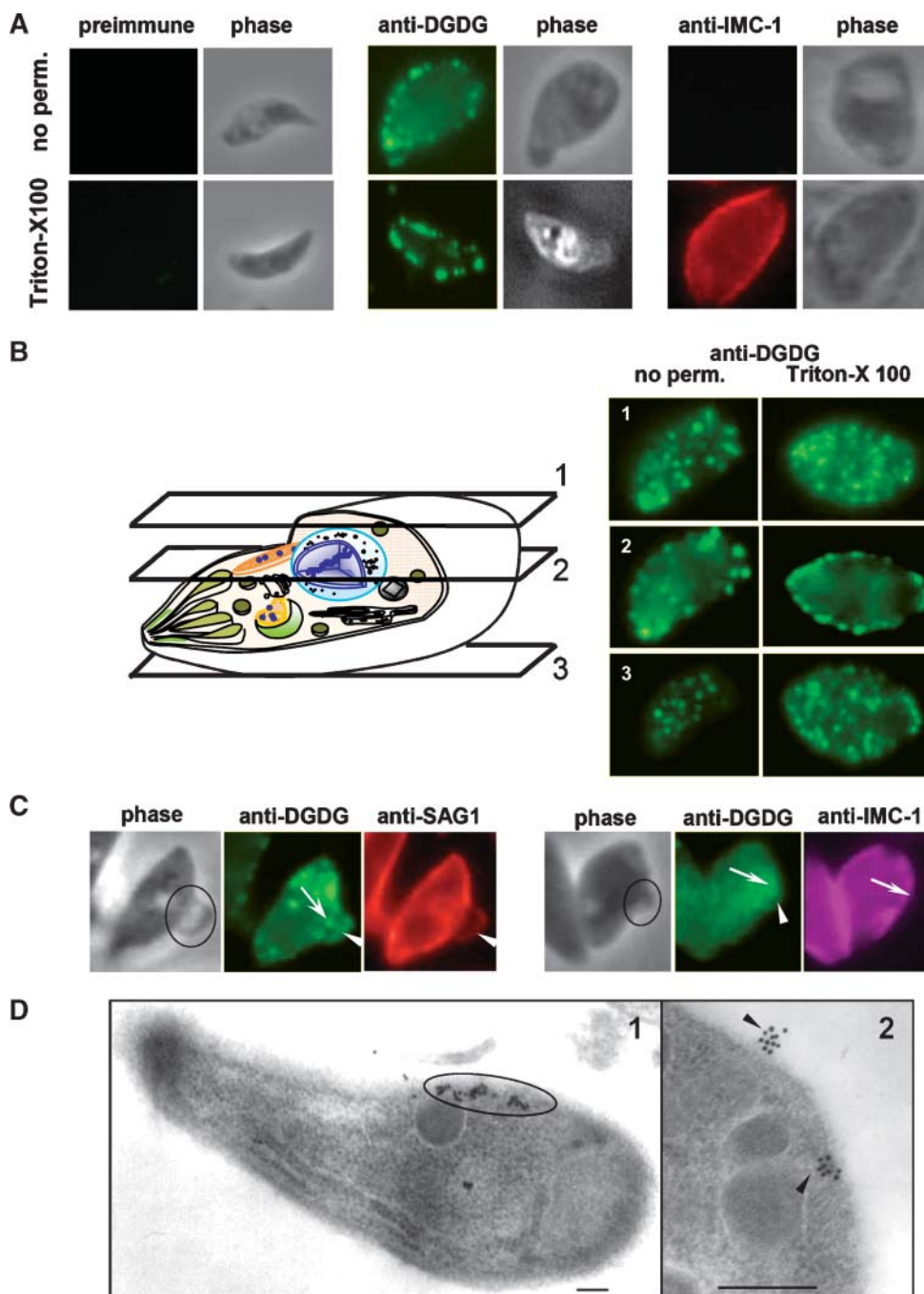
Fig. 2. Immunolocalization of DGLE in extracellular *T. gondii* tachyzoites. A: IF analysis of DGLE in extracellular parasites. Freshly lysed tachyzoites were labeled with rabbit preimmune (left) or anti-DGDG (center and right) serum without any fixation and permeabilization (no perm.) and then observed by epifluorescence. In parallel, parasites were fixed, permeabilized with Triton X-100, and then labeled with anti-DGDG (Triton X-100). The absence of labeling with anti-IMC-1 was used as a control for the absence of cell permeabilization. B: Three-dimensional distribution of DGLE in extracellular *T. gondii*. Immuno-fluorescence was analyzed by adjustment of imaging focus at the top (1), medial (2), or bottom (3) sections of the same parasite. DGLE is detected as microdomains at the parasite periphery. C: IF analysis of DGLE in the plasma membrane and inner membrane complex after pellicle physical membrane separation. Parasites were treated with 1% glycerol for 1 h, allowing physical separation of the plasma membrane (arrowheads) from the inner membrane complex (arrows) and producing plasma membrane blebs (circles). Treated parasites were colabeled with both monoclonal anti-SAG1 antibody (red) and rabbit anti-DGDG serum (green) or with both rabbit anti-IMC1 (purple) and rat anti-DGDG (green) sera. D: Immunogold labeling of extracellular parasites with rabbit anti-DGDG serum. 1, Labeling at the level of the pellicle (circle). 2, Dotted labeling at the surface of the plasma membrane and at the level of the inner membrane complex (arrowheads). Bars = 500 nm.

(colabeling with antibodies raised against the surface protein SAG1) and the inner membrane complex (colabeling with antibodies raised against IMC-1). When freshly isolated parasites were immunogold-labeled with the rabbit anti-DGDG serum, DGLE was consistently detected at the cell periphery (Fig. 2D, panel 1) and exposed at the plasma membrane surface or within the inner membrane complex (Fig. 2D, panel 2).

To assess the localization of DGLE in the pellicle, extracellular parasites were fractionated on sucrose gradients (45) to obtain pellicle-enriched fractions (**Fig. 3A**). Proteins from these fractions were analyzed by Western blot using compartment markers: clear enrichments in both SAG1 and IMC1 were observed in the pellicle fraction (Fig. 3A). When lipids were extracted, spotted onto nitrocellulose, and probed with the rabbit anti-DGDG serum, DGLE was immunodetected (Fig. 3A). DGLE represented ∼0.5% of the total lipid content of the pellicle fractions (Fig. 1F).

Attempt to assess the structure of DGLE by mass spectrometry lipidomic analysis of the pellicle membranes purified from extracellular *Toxoplasma*

We analyzed the lipid profile of the pellicle-enriched fraction by mass spectrometry and attempted to identify DGLE candidate(s) in the minor peaks corresponding to accurate glycolipidic structures (Fig. 3B). The amounts of the main phospholipids, and *Toxoplasma*-specific enrichment in phosphoethanolamine ceramide, confirmed previous analyses performed on whole parasites (13, 24). Based on immunoblot analyses, the proportion of lipids reacting with the antisera was estimated to be in the range of 1.2–6 nmol/mg total glycerolipids. Immunolabeling of DGLE is consistent with *1*) the occurrence of DGDG but also with *2*) digalactolipids having an alternative hydrophobic moiety (i.e., acylalkylglycerol or ceramide; Fig. 3B) and *3*) dihexosyl lipids that might be cross-detected by the antibody but harboring different sugars, such as Glc, GalNAc, or GlcNAc. Furthermore, we cannot exclude the possibility that antibodies react with *4*) more complex glycolipids terminated by a dihexosyl group. Here, we particularly examined nonsubstituted monohexosyl and dihexosyl lipids. Scans for neutral loss of 179 [i.e., loss of ammoniated hexose minus water ($C_6H_{13}O_5N$)] or neutral loss of 341 [i.e., loss of ammoniated dihexose minus water ($C_{12}H_{23}O_{10}N$)] produced a few peaks close to the detection thresholds in the MGDG/MGAAG (700–900) or DGDG/DGAAG (890–1,050) mass ranges, respectively. In the neutral loss 179 scan, consistent with the loss of one hexosyl residue, minor peaks were detected at m/z 732, 734, 760, 764, 776, 792, and 804. In the neutral loss 341 scan, consistent with the loss of two hexosyl residues, minor peaks were detected at m/z 894, 896, 908, 910, 922, 936, 954, and 966. These weak peaks might be attributable to the occurrence of hexosyl diacyl lipids in the sample in the low picomole range, consistent with the quantity detected in the immunostaining dot-blot experiments. Some of the weak peaks, including those at m/z 894, 896, and 922, are distinct from the standard

galactolipids and could correspond, as $[M + NH_4]^+$, to alk(en)yl-acyl dihexosylglycerolipids.

In contrast with glycosylated glycerolipids, the monohexosylceramides and dihexosylceramides were detected in higher quantity (Fig. 3B). Among dihexosylceramides, digalactosylceramide could contribute to the binding of anti-DGDG antibodies, particularly if the digalactosyl conformation resembles that of the DGDG polar head [α-galactosyl(1→6)β-galactose].

Although the low abundance of DGLE is a technical limitation for global characterization, in the range of low-level contamination in the mass spectrometer, so that no conclusive result could be drawn regarding the structure of the DGLE hydrophobic moiety, mass spectrometry lipidomic analyses indicate the clear presence of dihexosyl lipids with a ceramide moiety and allow for the possibility of other hydrophobic moieties (DAG, acylalkylglycerol) at low levels. Any of these structures may represent the DGLE that reacts with the anti-DGDG antibodies.

During host cell invasion and endodyogenic multiplication, DGLE relocates to the anterior tip of the *Toxoplasma* cells

Localization of DGLE was analyzed during intracellular parasite development. **Figure 4A** shows that the preimmune serum did not react with human or *Toxoplasma* cells. Because the parasite population was not synchronized at the time of host cell invasion, different stages of parasite development were observed on the same slide at 24 h after infection. Figure 4B summarizes these observations. At the time of host cell invasion, when the parasite squeezes through the moving junction (51), a relocalization of DGLE was observed. At the posterior end of the parasite (Fig. 4B, panel 1), which was still outside the host cell, a dotted labeling was observed, reminiscent of that observed at the surface of extracellular parasites (Fig. 2). By contrast, concentration of DGLE was observed in the apical part of the parasite, which was already inside the intracellular forming vacuole. Early after vacuole formation, *Toxoplasma* is known to accumulate at its posterior end the dense granule protein GRA2 (4). Colabeling of recently invaded parasites with anti-DGDG rabbit antibodies, a monoclonal anti-GRA2, and Hoechst reagent showed that DGLE was concentrated opposite to GRA2 (i.e., at the anterior part of the parasite) (Fig. 4C). Together, Fig. 4B, C show that after invasion and the formation of the parasitophorous vacuole, DGLE relocates rapidly to the anterior tip of the parasite.

During the first division of the parasite (Fig. 4B, panel 2), DGLE remained concentrated as a gradient at the anterior of the mother cell and was also detected in duplicated structures at the apex of the daughter cells. Colabeling with anti-DGDG rat serum and monoclonal anti-IMC1 (Fig. 4D) showed that DGLE did not fully overlap with IMC1, the localization of which follows the complete inner membrane complex of daughter cells (Fig. 4D, arrowheads). Therefore, anti-DGDG/anti-IMC1 colabeling highlights a gradient of DGLE at the anterior part of the inner membrane complex. DGLE participation in apical pole devel-
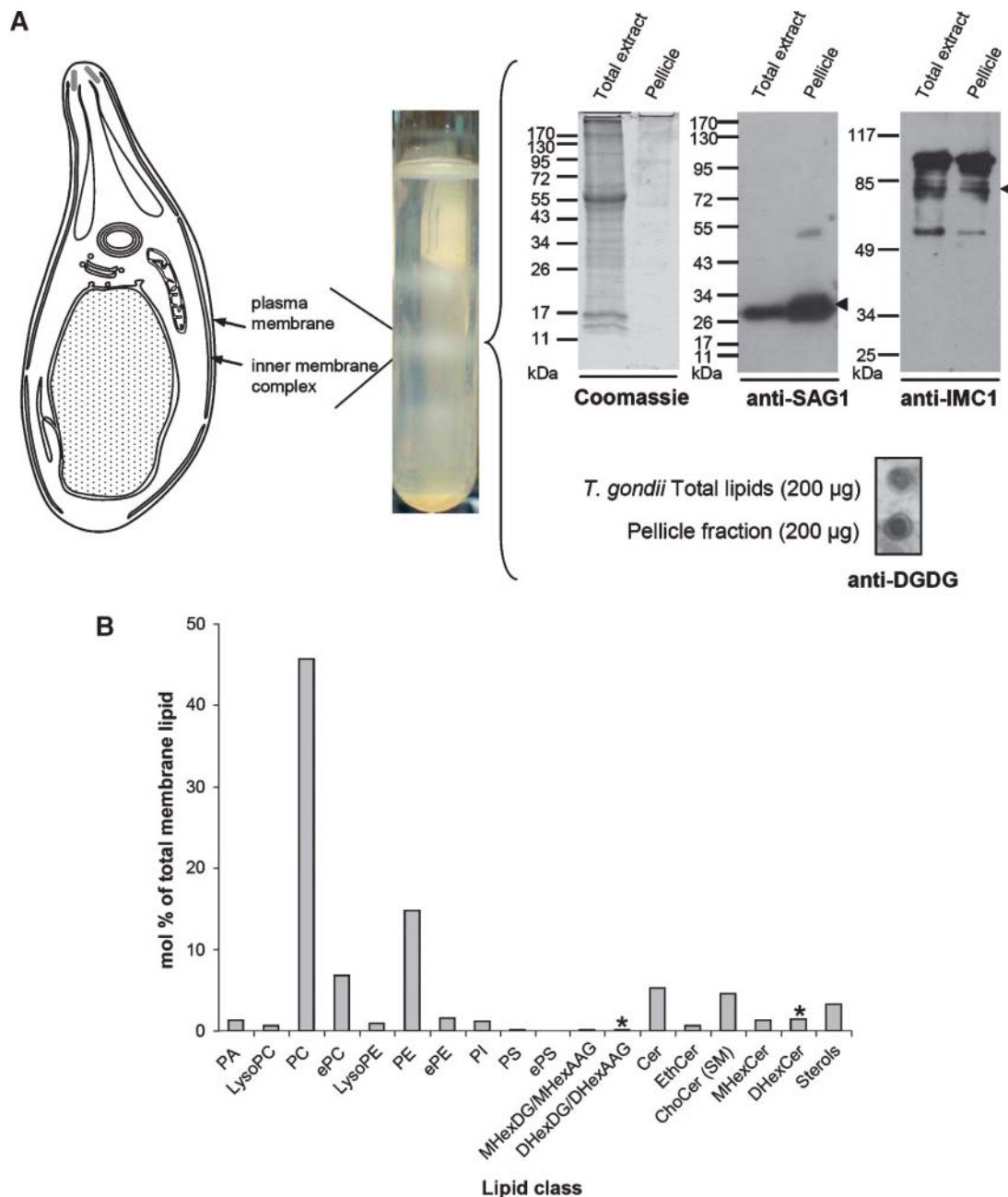
Fig. 3. Lipid analyses of pellicle fractions purified from extracellular *T. gondii* tachyzoites. A: Purification of pellicle membranes. Pellicle membranous structures were fractionated from extracellular *T. gondii* tachyzoites (scheme at left) after isopycnic centrifugation on a saccharose gradient (center). Enrichment in pellicle-specific proteins (Pellicle) was assessed by immunoblot analysis using plasma membrane and inner membrane complex markers (i.e., monoclonal anti-SAG1 and rabbit anti-IMC1 serum). Loaded samples (Total extract and Pellicle) correspond to the same initial amount of unfractionated and fractionated parasites (10^8 parasites). Lipids were extracted and 200 μg was analyzed by immunoblot with rabbit anti-DGDG serum. B: Lipid profile of *Toxoplasma* pellicle membranes. Polar lipids from pellicle membranes were analyzed by mass spectrometry and quantified based on known amounts of internal standards for each lipid class. Sterols (including cholesterol and steryl esters) were quantified by a resofurin-based fluorometric assay. The histogram gives average values of two series of quantifications. Glycosylated lipids were analyzed based on the presence of one or two hexosyl residues on the polar head, consistent with the structure of one or two galactosyl residues. Lipids that might terminate by an α-galactosyl(1→6)galactose and be detected by anti-DGDG antibodies are labeled with asterisks. Amounts of MHexDG/MHexAAG, DHexDG/DHexAAG, and PA include weak peaks corresponding to structures that were not verifiable as belonging to these classes. PA, phosphatidic acid; LysoPC, lyso-phosphatidylcholine; ePC, ether-linked PC [i.e., alk(en)yl, acyl PC]; LysoPE, lyso-phosphatidylethanolamine; ePE, ether-linked PE [i.e., alk(en)yl, acyl PE]; PI, phosphatidylinositol; PS, phosphatidylserine; ePS, ether-linked PS [i.e., alk(en)yl, acyl PS]; MHexDG, monohexosyldiacylglycerol (including MGDG); MHexAAG, monohexosyl-alk(en)yl-acyl glycerol (including MGAAG); DHexDG, dihexosyldiacylglycerol (including DGDG); DHexAAG, dihexosyl-alk(en)yl-acyl glycerol (including DGAAG); Cer, ceramide; EthCer, phosphoethanolamine ceramide; ChoCer; phosphocholine ceramide or SM; MHexCer, monohexosylceramide (including galactosylceramide); DHexCer, dihexosylceramide (including digalactosylceramide).
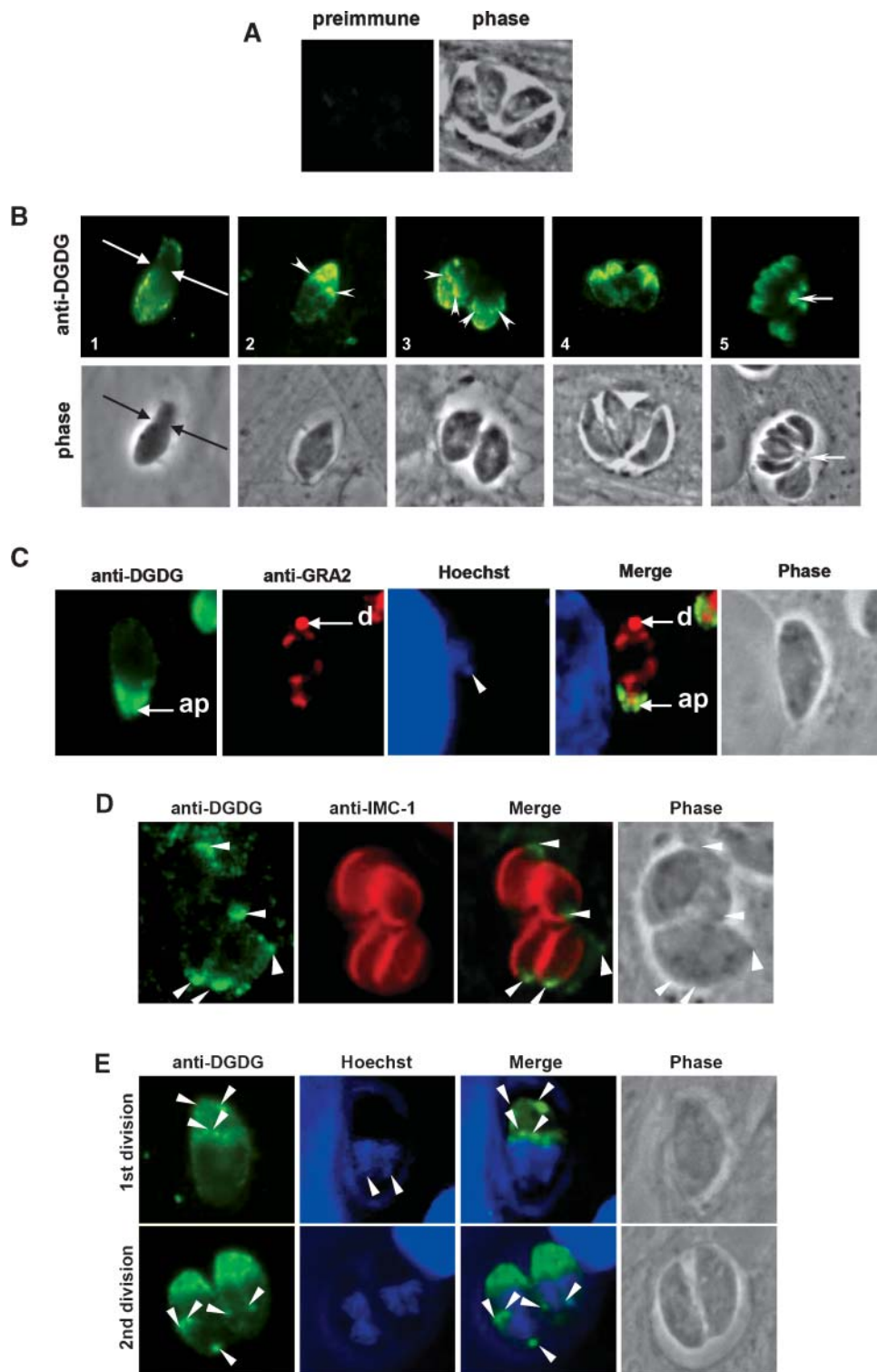
Fig. 4. Immunolocalization of DGLE in intracellular parasites. A: Immunostaining of intracellular parasites with preimmune serum. B: Sequence of intracellular parasites labeled with rabbit anti-DGDG. 1, Arrows indicate the moving junction. 2, 3, Arrowheads indicate the anterior tip of daughter parasites forming within the mother cell. 5, The arrow shows the intravacuolar residual body. C: Parasites recently invaded (<1 h) and colabeled with rabbit serum anti-DGDG, monoclonal anti-GRA2, and Hoechst reagent. ap, anterior part of the intracellular parasite; d, posterior GRA2 dot. The arrowhead indicates the apicoplast nucleic content. D: Colabeling of dividing intracellular parasites with both rat anti-DGDG serum and rabbit anti-IMC1 serum. Arrowheads indicate the anterior part of parasites, including those of daughter cells. E: Colabeling of dividing parasites with rabbit anti-DGDG serum and Hoechst reagent. Arrowheads indicate localizations where DGLE is concentrated in dividing parasites.

opment was further supported by superimposition of the divided nucleus and the anti-DGDG labeling shaping the future apical inner membrane complex of daughter parasites (Fig. 4E). During the subsequent rounds of division (Fig. 4B, panels 3–5), DGLE localization was similar, at the anterior tips of the parasites and of their dividing daughter cells. After division, parasites remain attached to each other by a vacuolar structure known as the residual body, which contains remnants of the mother parasites (52). Within the vacuolar compartment, DGLE was detected at the level of this residual body but was not detected in any other vacuolar membrane, as shown by IF (Fig. 4B, panel 5).

DGLE localization in membrane domains of the parasite pellicle is affected by the depolymerization of parasite actin

Because DGLE was localized in patches at the parasite periphery of extracellular parasites and at the anterior tip of intracellular parasites, where it remained during endodyogeny, we addressed the question of a possible clustering of DGLE in DRMs (or rafts) and the potential relation with the parasite cytoskeleton.

DRMs were isolated from extracellular parasites, according to the protocol recently reported by Azzouz et al. (48). Sterol and steryl ester quantification demonstrated a consistent enrichment in the DRM fraction (11.35 mol% of the membrane lipids) compared with the pellicle fraction (3.3 mol%). When lipid extract from the DRM fraction was spotted onto nitrocellulose and incubated with the rabbit anti-DGDG serum, DGLE was detected: the DGLE content of the DRM fraction was estimated at ∼0.1%, based on the intensity of the immunostaining with anti-DGDG antibodies (Fig. 1F). Because this proportion is lower than that of pellicle lipids (i.e., 0.5%) (Fig. 1F), this analysis shows that the DGLE membrane domains visualized by imaging experiments do not coincide strictly with sterol-rich DRMs.

To characterize the possible relation of DGLE membrane domains with the cytoskeleton, various treatments with cytoskeleton-destabilizing drugs, either depolymerizing microtubules (oryzalin) or actin (cytochalasin D) or affecting myosin A (butanedione monoxime), were carried out before DGLE visualization (**Fig. 5A, B**). Oryzalin or butanedione monoxime treatment did not change the distribution of DGLE at the anterior part of the parasite (Fig. 5A, left and central panels). By contrast, treatment of infected cells with cytochalasin D resulted in the redistribution of DGLE to the periphery of the cell (Fig. 5A, right panel). These results suggest that DGLE might be directly or indirectly linked to parasite polymerized actin, which is atypically localized between the plasma membrane and the inner membrane complex in Apicomplexa (53), and that DGLE does not interact with microtubules or myosin A.

Actin filaments are particularly difficult to observe in apicomplexan parasites (53). Nevertheless, filamentous actin was recently detected as short filaments located between the subpellicular network and the plasma membrane of *Toxoplasma* (44). When preparations of parasite subpellicular network, known to preserve both microtubules and filamentous actin, were incubated with the rabbit anti-DGDG serum, labeling was observed at the extreme tip of the conoid (Fig. 5C, panels 1, 2), along the subpellicular microtubules (Fig. 5C, panel 3), and along the whole cell surface (Fig. 5C, panels 4, 5). These observations further support a possible association of DGLE with parasite filamentous actin.

Search for DGLE in other apicomplexan parasites

We examined the possible occurrence of DGLE in other apicomplexan parasites (**Fig. 6**). A distribution pattern similar to that observed in *Toxoplasma* was detected in the closely related apicomplexan parasite *N. caninum* (Fig. 6A). DGLE was also detected in *C. parvum*, an Apicomplexa without plastid (Fig. 6B). In *P. falciparum*, the main malarial parasite, DGLE was detected, with a subcellular localization that appeared to be remodeled along parasitic stages in the human host (Fig. 6C). In ring stages, DGLE showed a crescent-like distribution as marginal or peripheral dots (Fig. 6C, panels 1, 2). Trophozoite-stage parasites (Fig. 6C, panel 3) exhibited DGLE domains at the cell periphery. A localization of the DGLE at the level of the developing merozoite membranes was then observed in the schizont-stage parasites (Fig. 6C, panels 4, 5). Eventually, an inner membrane complex-like distribution was observed in the gametocyte stage, with a regular network of superficial dots (Fig. 6C, panel 6). We further detected DGLE in *Babesia divergens* (data not shown). We did not detect DGLE in *Trypanosoma brucei*, a nonapicomplexan unicellular parasite (data not shown). Together, these results show that the anti-DGDG serum labels a lipid found in numerous parasites of the Apicomplexa phylum. In all cases, DGLE appears to be clustered in membrane domains at the cell periphery and to be mobilized at the anterior tip upon invasion.

DISCUSSION

The presence of a plastid in *Toxoplasma* suggested that MGDG and DGDG, the main chloroplast and cyanobacteria lipids (27–29), might also be important constituents of the apicoplast membranes. In plants and algae, MGDG and DGDG are synthesized within plastid envelope membranes (29, 31, 54–58). In plants, MGDG is produced by the galactosylation of DAG, whereas it is generated by a two-step glucosylation and epimerization in cyanobacteria (59). In both plants and cyanobacteria, DGDG is formed by the addition of a galactosyl residue to MGDG (29, 54). Upon phosphate deprivation, DGDG is exported outside plastids to the plasma membrane (60) and the mitochondria (31). No MGDG synthase or DGDG synthase homologous sequences could be detected in the genome of some plastid-containing organisms, such as *Euglena*, in which MGDG and DGDG are well-established constituents (61), suggesting that their synthesizing enzymes might have strongly diverged during evolution. Searching both *Toxoplasma* and *Plasmodium* databases did not reveal any gene candidate for MGDG synthesis, leaving the question of the monogalactolipid-synthesizing enzymes unresolved. A
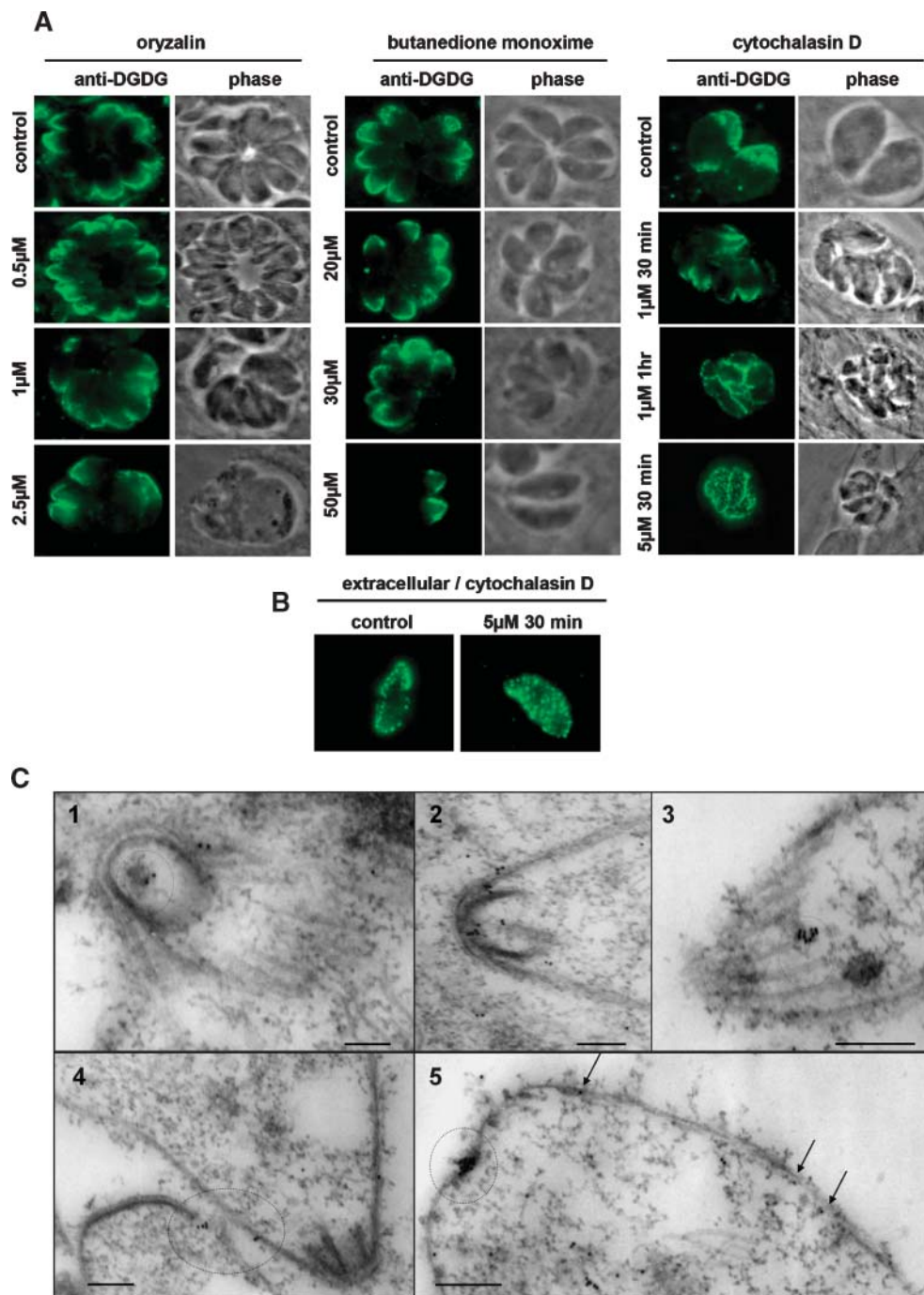
Fig. 5. Analysis of the relation between DGLE pellicle membrane domains and the *T. gondii* cytoskeleton. A: Evolution of DGLE pellicle membrane domains after chemical impairment of the *T. gondii* cytoskeleton of intracellular tachyzoites with oryzalin, butanedione monoxime, and cytochalasin D. Infected cells were treated with oryzalin, a tubulin-destabilizing agent, butanedione monoxime, a myosin A binding drug, or cytochalasin D, an actin-depolymerizing factor. After labeling with rabbit anti-DGDG serum, a relocalization of DGLE similar to that observed in extracellular parasites was observed only under conditions in which actin filaments were disrupted. DGLE membrane domains formed spontaneously after the cytochalasin D time course. B: Evolution of DGLE pellicle membrane domains after treatment of the *T. gondii* cytoskeleton of extracellular tachyzoites with cytochalasin D. Extracellular parasites were treated with 5 µM cytochalasin D for 30 min and labeled with rabbit anti-DGDG serum. No apparent change in DGLE localization was observed. C: Immunogold labeling of the parasite subpellicular network with the rabbit anti-DGDG serum. Immunolocalization of DGLE in cytoskeletal preparations was carried out as described (44). DGLE is concentrated mainly at the extreme tip of the conoid (1, circle) as well as along the inner membranes, in close proximity to subpellicular microtubules, which are preserved after detergent treatment (2–4, arrows and circles). DGLE was also found concentrated at the posterior end (5, circle). Bars = 200 nm.
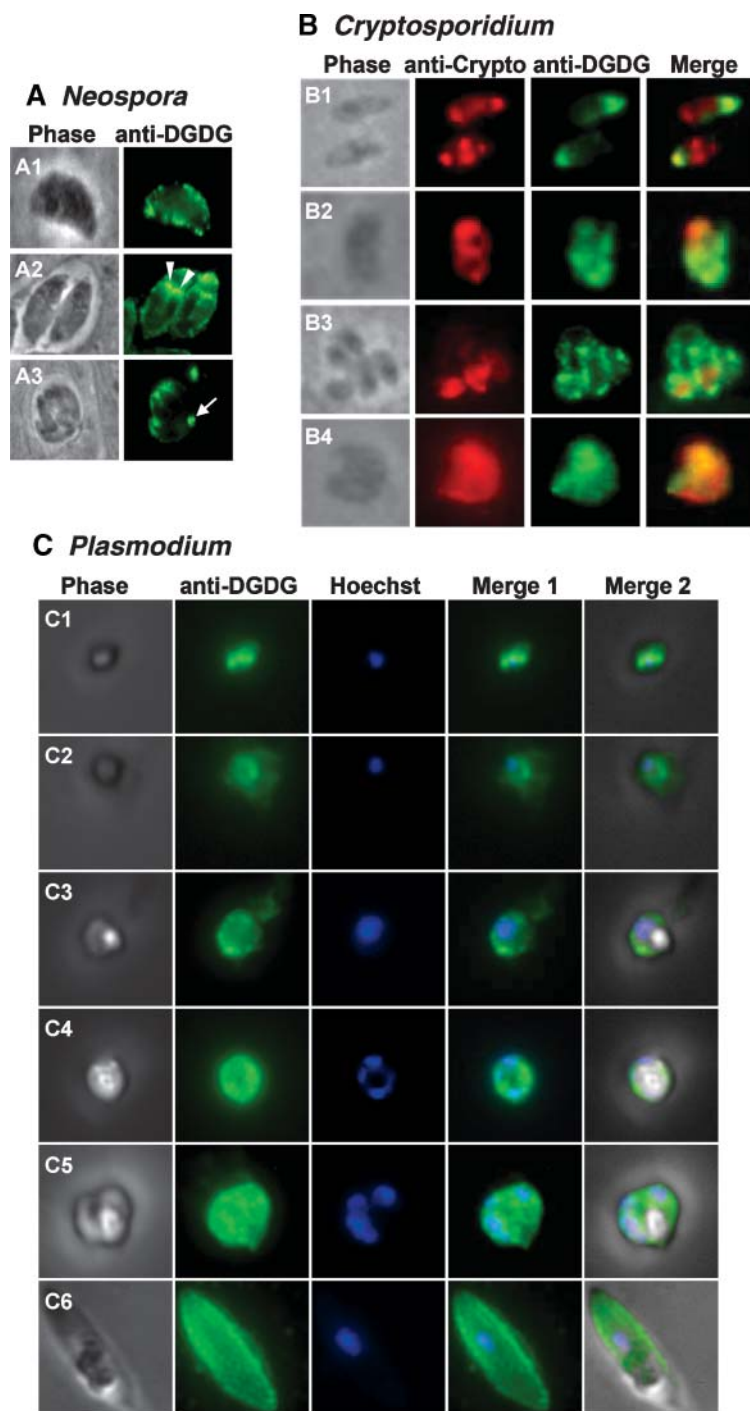
A Neospora

Phase anti-DGDG

B Cryptosporidium

Phase anti-Crypto anti-DGDG Merge

C Plasmodium

Phase anti-DGDG Hoechst Merge 1 Merge 2

Fig. 6. Localization of DGLE in *N. caninum*, *C. parvum*, and *P. falciparum*. A: Immunolabeling of *N. caninum* tachyzoites with rabbit anti-DGDG serum. A1, Recently invaded tachyzoite. A2, Replicating pair of parasites. A3, Vacuole containing four parasites. Arrowheads indicate the newly formed parasites within the mother cell; the arrow shows the intravacuolar residual body. B: Immuno-labeling of *C. parvum* cells with both rabbit anti-DGDG serum and rat anti-*Cryptosporidium* serum. B1, Extracellu-lar sporozoites exhibiting an apical distribution of DGLE. B2, B3, DGLE localization at the periphery of intracellular sporozoites, with stronger presence at the apical pole. B4, Distribution of DGLE at the membrane of the meront-stage parasites. C: Distribution of DGLE during the asex-ual cycle of *P. falciparum*. Cultures of *P. falciparum*-infected red blood cells were fixed and permeabilized using Triton X-100. Immunolabeling was performed using anti-DGDG antibody, and nuclei were stained with Hoechst 33258. Acquisitions were ordered according to the life stage of the parasites. C1, C2, A crescent-like distribution of DGLE as marginal dots was observed in the ring stages. C3, The DGLE distribution is localized as peripheral dots close to the membranes of the trophozoite-stage parasites. C4, C5, Reorganization of DGLE to the developing merozoite membranes in schizont-stage parasites. C6, An inner mem-brane complex-like distribution as well as reticulated su-perficial dots were observed in the gametocyte stage.

single gene in *Toxoplasma* (49.m00002; PF10_0316 in *P. falciparum*), coding for a 624 amino acid protein, contains a 387 amino acid segment with ∼24% identity with cyano-bateria dgdA, a 389 amino acid DGDG synthase (*Synechocystis* slr1508) (62), and also has strong homology with lipo-polysaccharide glycosyltransferases involved in glycosyl-phosphatidylinositol anchor synthesis. This gene might encode an enzyme of broad specificity catalyzing the syn-thesis of DGLE and should be functionally analyzed in the future.

Here, we used specific polyclonal antibodies from rabbit or rat, raised against plant DGDG, to investigate the oc-currence and cell dynamics of a class of lipids harboring a DGLE in *Toxoplasma* and other Apicomplexa. We did not detect any reactivity of any of the anti-DGDG antibodies with mammalian lipid extracts or cell membranes. Analysis of the anti-DGDG specificity assessed by nitrocellulose im-munostaining experiments (Fig. 1) shows that the anti-bodies have no significant cross-reactivity with *Toxoplasma* proteins and that they do not specifically bind to the hydrophobic moiety of DGDG (i.e., the DAG structure). Because preincubation of the antibodies with DGDG com-petes with both chloroplastic and *Toxoplasma* lipids, a strong structural similarity to the polar head of DGDG seems

required for the antibody binding. Based on these analyses, DGLE detected in *Toxoplasma* lipid extracts is possibly a dihexosyl lipid whose polar head is close to an α-galactosyl(1→6)β-galactose and, based on previous metabolic analyses (24, 30), whose hydrophobic moiety contains at least one hydrolyzable acyl ester (30). We do not exclude the possibility that other lipid structures, with a more complex polar head terminated by a dihexosyl group, might also be detected using anti-DGDG antibodies.

Inconsistent with the initial idea sustaining the search for chloroplast galactolipids in Apicomplexa, none of our IF or IEM experiments allowed the detection of DGLE in an internal structure of *Toxoplasma* that resembles the apicoplast. Galactolipid lower abundance, epitope distribution, or access of antibodies to internal membranes might not allow immunodetection in this organelle (Fig. 4C). Galactolipids might be synthesized by apicoplast enzymes but rapidly exported to other cell compartments, in a similar manner to which DGDG is exported outside chloroplasts in phosphate-deprived plants (31, 60). Alternatively, evolution of the galactolipid synthetic machinery might have occurred with relocation outside the apicoplast, or it may be completely independent on any chloroplast-related process. In extracellular life stages of *Toxoplasma*, DGLE was detected at the periphery of the cell by both IF and IEM imaging, partly exposed at the surface of the plasma membrane (Fig. 2A, B, D), but also in the inner membrane complex (Fig. 2C, D). Localization in pellicle membranes was confirmed by immunostaining of lipid extracts of pellicle-enriched fractions (Fig. 3A). Therefore, DGLE appears as a minor constituent of the pellicle of tachyzoites, with a dotted or patched pattern that suggests a concentration in membrane domains.

Upon invasion, DGLE relocates to the anterior part of the cell (Fig. 4). Interestingly, we could apparently reverse the relocation of DGLE by treating intracellular *Toxoplasma* with cytochalasin D, an actin-depolymerizing agent (Fig. 5A). This result suggests that DGLE relocation might be directly or indirectly determined by actin-dependent processes and that DGLE might be a factor of the invasion mechanism. In the current understanding of invasion, conserved multiprotein machineries are involved, including both the parasite acto-myosin motor located between the parasite plasma membrane and the inner membrane complex and the microneme secretory apparatus (44, 52, 63). During invasion, adhesive transmembrane proteins (secreted from micronemes) bind to the host cell. These adhesive proteins are linked to the invasive motor via an interaction between their cytoplasmic tail and aldolase, which in turn interacts with actin linked to myosin A. The unconventional myosin A is rigidly anchored to inner membrane complex proteins (IMC-1 and IMC-3) through an interaction with protein intermediates, which include the myosin A-interacting protein (MTIP in *Plasmodium* and MLC1 in *Toxoplasma*) and the gliding-associated proteins of 45 and 50 kDa (GAP45 and GAP50). The cytosolic face of the inner membrane complex is then associated directly with 22 subpellicular microtubules, which maintain the parasite shape

and which are also involved in the cell-gliding motility (44, 52, 63). Therefore, DGLE that rapidly moves to the anterior part of the cell during invasion might be associated with some of these constituents, an hypothesis further supported by IEM detection of DGLE in the vicinity of cytoskeleton structures (Fig. 5C). Because the DGLE gradient was not disorganized by oryzalin, a tubulin-destabilizing agent, or butanedione monoxime, affecting myosin A (Fig. 5A), our study suggests that during invasion DGLE might be associated with actin and/or micronemal proteins. Alternatively, Johnson et al. (64) recently showed that GAP50 and the myosin complex are immobilized within the inner membrane complex at the level of DRM domains, which are enriched in sterols and have a higher density than DRMs classically reported in eukaryotic cells. DGLE might be a component of such inner membrane complex DRMs.

Toxoplasma division is a binary process called endodyogeny during which a single chromosome replication is followed by concurrent mitosis and parasite budding (65). In our study, DGLE was detected within dividing cells at the tip of the duplicated inner membrane complexes of the daughter cells (Fig. 4). Because DGLE was also detected at the tip of the mother cell and as part of the residual body, the DGLE of the daughter cells is likely newly synthesized rather than recycled.

Attempts to determine the precise structure of DGLE by mass spectrometry analyses of the pellicle membranes (Fig. 3B) allowed us to inventory some minor lipids, particularly dihexosyl lipids with various hydrophobic moieties (ceramides, DAG, acylalkylglycerol), that might react with the anti-DGDG antibodies. Immunolabeling of DGLE is consistent with the occurrence of DGDG, and/or digalactolipids having an alternative hydrophobic moiety (i.e., acylalkylglycerol or ceramide; Fig. 3B), and/or dihexosyl lipids that might be cross-detected by the antibody but harboring different sugars, such as Glc, GalNAc, or GlcNAc. Furthermore, we cannot exclude the possibility that antibodies react with more complex glycolipids terminated by a dihexosyl group. Whereas dihexosyl ceramides could be unambiguously assessed, peaks corresponding to dihexosyl DAG or dihexosyl acylalkylglycerol were close to the detection threshold, and no conclusive result could be drawn regarding the unambiguous determination of the DGLE structure. Previous reports of the metabolic labeling of a lipid comigrating with DGDG after incubation with radiolabeled UDP-galactose (30) and acetate (24) support the idea that the DGLE hydrophobic moiety is DAG or acylalkylglycerol. Because numerous glycolipids generated by the same enzyme can share an identical polar head but harbor different hydrophobic moieties (e.g., MGCB and MGDG generated by galacto-cerebroside synthase based on the supplied substrate, ceramide or DAG, respectively), the possibility that the detected DGLE corresponds to glycosyl glycerolipids or glycosyl ceramides or to both classes cannot be rigorously excluded. Recently, the parasitic trematode *Fasciola hepatica* was shown to exhibit mammalian-type glycolipids, including α-galactosyl(1→4)β-galactose- and α-galactosyl

(1→3)β-galactose-terminating glycoceramides, as well as nonmammalian β-galactosyl(1→6)β-galactose-terminating glycoceramides that account for cestode serological cross-reactivity (66). It is possible, therefore, that like glycolipids of the neogala series [i.e., β-galactosyl(1→6)β-galactose], the α-galactosyl(1→6)β-galactose-terminating glycolipids might be related to the pathogenic process.

We also attempted to refine the distribution of DGLE in membrane domains by analyzing the lipid content of DRMs. In a recent report, DRMs isolated from the pellicle of extracellular parasites were shown to be enriched in cholesterol, GM1 ganglioside, SM, phospholipids, and still unidentified lipids. They were also shown to be associated with proteins involved in invasion and motility, suggesting their localization at the inner membrane complex (53). Here, DRM fractions purified according to the same procedure were enriched in sterols and contained DGLE, although no specific enrichment in DGLE could be measured (Fig. 1F). The galactosyl head groups of lipids are known to interact and promote the organization of stacked domains (67). Therefore, DGLE might spontaneously form membrane domains, possibly associated with DRMs, with some specific cellular functions including protein anchoring. Thus, the actin-dependent migration of DGLE to the anterior part of the parasite, occurring during early infection processes, might be part of a mechanism recruiting other components to the apex of the cell.

DGLE was detected in important apicomplexan parasites (*Toxoplasma*, *Neospora*, *Plasmodium*, *Babesia*, and *Cryptosporidium*) (Fig. 6). In all cases, DGLE was localized at the periphery of the cell, either as pellicle membrane domains or as an apical gradient. This study shows that DGLE is found broadly in the Apicomplexa phylum, in both apicoplast-containing (*Toxoplasma*, *Neospora*, *Plasmodium*, and *Babesia*) and apicoplast-free (*Cryptosporidium*) species. If DGLE synthesis derived from an ancestral chloroplastic DGDG synthetic machinery, this result suggests that the corresponding enzymes are no longer localized within a plastid, at least in *Cryptosporidium*.

After this descriptive work, future studies include the precise characterization of the hydrophobic moiety of DGLE, requiring very large-scale cultures of the parasites, lipid class purification, and analysis. Although this work was motivated by the analysis of chloroplast galactolipids in Apicomplexa, based on a series of experimental evidence, technical limitations did not allow us to give any definitive demonstration regarding the occurrence of these precise lipidic structures in Apicomplexa. It becomes clear that the analysis of apicoplast lipids requires a purification procedure for this organelle, respecting its membrane integrity. The current understanding of galactolipid synthesis in plastid-containing organisms is still incomplete, lacking some of the enzymes in important photosynthetic organisms that might be helpful to explore Apicomplexa genomes. In spite of the apparently small number of glycosyltransferases in Apicomplexa [as inventoried in the CAZy database (68)], genes sharing some similarity with cyanobacteria dgdA can be detected, and efforts should focus on their analyses and on the search for other glycolipid-synthesizing enzymes to functionally advance our understanding of simple glycolipid classes in the context of Apicomplexa pathogeneses.

REFERENCES

1. Håkansson, S., A. J. Charron, and L. D. Sibley. 2001. *Toxoplasma* evacuoles: a two-step process of secretion and fusion forms the parasitophorous vacuole. *EMBO J.* **20:** 3132–3144.
2. Mordue, D. G., N. Desai, M. Dustin, and L. D. Sibley. 1999. Invasion by *Toxoplasma gondii* establishes a moving junction that selectively excludes host cell plasma membrane proteins on the basis of their membrane anchoring. *J. Exp. Med.* **190:** 1783–1792.
3. Charron, A. J., and L. D. Sibley. 2004. Molecular partitioning during host cell penetration by *Toxoplasma gondii. Traffic.* **5:** 855–867.
4. Mercier, C., K. D. Z. Adjogble, W. Däubener, and M. F. Cesbron-Delauw. 2005. Dense granules: are they key organelles to help understand the parasitophorous vacuole of all Apicomplexa parasites? *Int. J. Parasitol.* **35:** 829–849.
5. Mordue, D. G., and L. D. Sibley. 1997. Intracellular fate of vacuoles containing *Toxoplasma gondii* is determined at the time of formation and depends on the mechanism of entry. *J. Immunol.* **159:** 4452–4459.
6. Keeley, A., and D. Soldati. 2004. The glideosome: a molecular machine powering motility and host-cell invasion by Apicomplexa. *Trends Cell Biol.* **14:** 528–532.
7. Dubremetz, J. F. 2007. Rhoptries are major players in *Toxoplasma gondii* invasion and host cell interaction. *Cell. Microbiol.* **9:** 841–848.
8. McFadden, G. I., M. E. Reith, J. Munholland, and N. Lang-Unnasch. 1996. Plastid in human parasites. *Nature.* **381:** 482.
9. Köhler, S., C. F. Delwiche, P. W. Denny, L. G. Tilney, P. Webster, R. J. Wilson, J. D. Palmer, and D. S. Roos. 1997. A plastid of probable green algal origin in apicomplexan parasites. *Science.* **275:** 1485–1489.

10. Ferguson, D. J. P., F. L. Henriquez, M. J. Kirisits, S. P. Muench, S. T. Prigge, D. W. Rice, C. W. Roberts, and R. McLeod. 2005. Maternal inheritance and stage specific variation of the apicoplast in *Toxoplasma gondii* during development in the intermediate and definitive host. *Eukaryot. Cell.* **4:** 814–826.

11. Wilson, I. 1993. Plastids better red than dead. *Nature.* **366:** 638.

12. Van Dooren, G. G., R. F. Waller, K. A. Joiner, D. S. Roos, and G. I. McFadden. 2000. Traffic jams: protein transport in *Plasmodium falciparum*. *Parasitol. Today.* **16:** 421–427.

13. Welti, R., E. Mui, A. Sparks, S. Wernimont, G. Isaac, M. Kirisits, M. Roth, C. W. Roberts, C. Botté, E. Maréchal, and R. McLeod. 2007. Lipidomic analysis of *Toxoplasma gondii* reveals unusual polar lipids. *Biochemistry.* **46:** 13882–13890.

14. Coppens, I., A. P. Sinai, and K. A. Joiner. 2000. *Toxoplasma gondii* exploits host low-density lipoprotein receptor-mediated endocytosis for cholesterol acquisition. *J. Cell Biol.* **149:** 167–180.

15. Waller, R. F., and G. I. McFadden. 2005. The apicoplast: a review of the derived plastid of apicomplexan parasites. *Curr. Issues Mol. Biol.* **7:** 57–79.

16. Zuther, E., J. J. Johnson, R. Haselkorn, R. McLeod, and P. Gornicki. 1999. Growth of *Toxoplasma gondii* is inhibited by aryloxyphenoxypropionate herbicides targeting acetyl-CoA carboxylase. *Proc. Natl. Acad. Sci. USA.* **96:** 13387–13392.

17. Gleeson, M. T. 2000. The plastid in Apicomplexa: what use is it? *Int. J. Parasitol.* **30:** 1053–1070.

18. McLeod, R., S. Muench, J. Rafferty, D. Kyle, E. Mui, M. Kirisits, D. Mack, C. Roberts, B. Samuel, R. Lyons, et al. 2001. Triclosan inhibits the growth of *Plasmodium falciparum* and *Toxoplasma gondii* by inhibition of apicomplexan Fab I. *Int. J. Parasitol.* **31:** 109–113.

19. Maréchal, E., and M. F. Cesbron-Delauw. 2001. The apicoplast: a new member of the plastid family. *Trends Plant Sci.* **6:** 200–205.

20. Roberts, C. W., R. McLeod, D. W. Rice, M. Ginger, M. L. Chance, and J. J. Goad. 2003. Fatty acid and sterol metabolism: potential antimicrobial targets in apicomplexan and trypanosomatic parasitic protozoa. *Mol. Biochem. Parasitol.* **126:** 129–142.

21. Muench, S., S. Prigge, M. J. Kirisits, R. McLeod, J. B. Rafferty, M. J. Kirisitis, C. W. Roberts, E. J. Mui, and D. Rice. 2007. Studies of *Toxoplasma gondii* and *Plasmodium falciparum* enoyl acyl carrier protein reductase and implications for the development of antiparasitic agents. *Acta Crystallogr. D Biol. Crystallogr.* **63:** 328–338.

22. Zhu, G. 2004. Current progress in the fatty acid metabolism in *Cryptosporidium parvum*. *J. Eukaryot. Microbiol.* **51:** 381–388.

23. Mazumdar, J., H. Wilson, E. Masek, C. A. Hunter, and B. Striepen. 2006. Apicoplast fatty acid synthesis is essential for organelle biogenesis and parasite survival in *Toxoplasma gondii*. *Proc. Natl. Acad. Sci. USA.* **103:** 13192–13197.

24. Bisanz, C., O. Bastien, D. Grando, J. Jouhet, E. Maréchal, and M. F. Cesbron-Delauw. 2006. *Toxoplasma gondii* acyl-lipid metabolism: de novo synthesis from apicoplast-generated fatty acids versus scavenging of host cell precursors. *Biochem. J.* **394:** 197–205.

25. Charron, A. J., and L. D. Sibley. 2002. Host cells: mobilizable lipid resources for the intracellular parasite *Toxoplasma gondii*. *J. Cell Sci.* **115:** 3049–3059.

26. Gupta, N., M. M. Zahn, I. Coppens, K. A. Joiner, and D. R. Voelker. 2005. Selective disruption of phosphatidylcholine metabolism of the intracellular parasite *Toxoplasma gondii* arrests its growth. *J. Biol. Chem.* **280:** 16345–16353.

27. Carter, H. E., R. H. McCluer, and E. D. Slifer. 1956. Lipids of wheat flour. I. Characterization of galactosylglycerol components. *J. Am. Chem. Soc.* **78:** 3735–3738.

28. Douce, R. 1974. Site of biosynthesis of galactolipids in spinach chloroplasts. *Science.* **183:** 852–853.

29. Maréchal, E., M. A. Block, A. J. Dorne, R. Douce, and J. Joyard. 1997. Lipid synthesis and metabolism in the plastid envelope. *Physiol. Plant.* **100:** 65–77.

30. Maréchal, E., N. Azzouz, C. S. de Macedo, M. A. Block, J. E. Feagin, R. T. Schwarz, and J. Joyard. 2002. Synthesis of chloroplast galactolipids in apicomplexan parasites. *Eukaryot. Cell.* **1:** 653–656.

31. Jouhet, J., E. Maréchal, B. Baldan, R. Bligny, J. Joyard, J., and M. A. Block. 2004. Phosphate deprivation induces transfer of DGDG galactolipid from chloroplast to mitochondria. *J. Cell Biol.* **167:** 863–874.

32. Martrou, P., M. Pestre, R. Loubet, A. Nicolas, and G. Malinvaud. 1965. La toxoplasmose congénitale (note concernant un cas mortel). *Limousin Med.* **53:** 3–7.

33. Trager, W., and J. B. Jensen. 1976. Human malaria parasites in continuous culture. *J. Parasitol.* **91:** 484–486.

34. Carter, R., L. Ranford-Cartwright, and P. Alano. 1993. The culture and preparation of gametocytes of *Plasmodium falciparum* for immunochemical, molecular, and mosquito infectivity studies. *Methods Mol. Biol.* **21:** 67–88.

35. Stokkermans, T. J., J. D. Schwartzman, K. Keenan, N. S. Morrissette, L. G. Tilney, and D. S. Roos. 1996. Inhibition of *Toxoplasma gondii* replication by dinitroaniline herbicides. *Exp. Parasitol.* **84:** 355–370.

36. Dobrowolski, J. M., and L. D. Sibley. 1996. *Toxoplasma* invasion of mammalian cells is powered by the actin cytoskeleton of the parasite. *Cell.* **84:** 933–939.

37. Mann, T., and C. Beckers. 2001. Characterization of the subpellicular network, a filamentous membrane skeletal component in the parasite *Toxoplasma gondii*. *Mol. Biochem. Parasitol.* **115:** 257–268.

38. Labruyère, E., M. Lingnau, C. Mercier, and L. D. Sibley. 1999. Differential membrane targeting of the secretory proteins GRA4 and GRA6 within the parasitophorous vacuole formed by *Toxoplasma gondii*. *Mol. Biochem. Parasitol.* **102:** 311–324.

39. Charif, H., F. Darcy, G. Torpier, M. F. Cesbron-Delauw, and A. Capron. 1990. *Toxoplasma gondii*: characterization and localization of antigens secreted from tachyzoites. *Exp. Parasitol.* **71:** 114–124.

40. Rodriguez, C., D. Afchain, A. Capron, C. Dissous, and F. Santoro. 1985. Major surface protein of *Toxoplasma gondii* (p30) contains an immunodominant region with repetitive epitopes. *Eur. J. Immunol.* **15:** 747–749.

41. Tomavo, S., B. Fortier, M. Soete, C. Ansel, D. Camus, and J. F. Dubremetz. 1991. Characterization of bradyzoite-specific antigens of *Toxoplasma gondii*. *Infect. Immun.* **59:** 3750–3753.

42. Gargala, G., A. Baishanbo, L. Favennec, A. François, J. J. Ballet, and J. F. Rossignol. 2005. Inhibitory activities of epidermal growth factor receptor tyrosine kinase-targeted dihydroxyisoflavone and trihydroxydeoxybenzoin derivatives on *Sarcocystis neurona*, *Neospora caninum*, and *Cryptosporidium parvum* development. *Antimicrob. Agents Chemother.* **49:** 4628–4634.

43. Sengupta, K., V. Hernández-Ramírez, A. Rios, R. Mondragón, and P. Talamás-Rohana. 2001. *Entamoeba histolytica*: Monoclonal antibody against b1 integrin-like molecule (140 kDa) inhibits cell adhesion to extracellular matrix components. *Exp. Parasitol.* **98:** 83–89.

44. Patron, A. S., M. Mondragon, S. Gonzalez, J. R. Ambrosio, A. L. B. Guerrero, and R. Mondragon. 2005. Identification and purification of actin from the subpellicular network of *Toxoplasma gondii* tachyzoites. *Int. J. Parasitol.* **35:** 883–894.

45. Lei, Y., D. Birch, M. Davey, and J. T. Ellis. 2005. Subcellular fractionation and molecular characterization of the pellicle and plasmalemma of *Neospora caninum*. *Parasitology.* **131:** 467–475.

46. Foussard, F., Y. Gallois, G. Tronchin, R. Robert, and G. Mauras. 1990. Isolation of the pellicle of *Toxoplasma gondii* (Protozoa, Coccidia): characterization by electron microscopy and protein composition. *Parasitol. Res.* **76:** 563–565.

47. Rabjeau, A., F. Foussard, G. Mauras, and J. F. Dubremetz. 1997. Enrichment and biochemical characterization of *Toxoplasma gondii* tachyzoite plasmalemma. *Parasitology.* **114:** 421–426.

48. Azzouz, N., H. Shams-Eldin, S. Niehus, F. Debierre-Grockiego, U. Bieker, J. Schmidt, C. Mercier, M. F. Cesbron-Delauw, J. F. Dubremetz, T. K. Smith, et al. 2006. *Toxoplasma* grown in human cells use GalNAc-containing GPI precursors to anchor plasma membrane proteins while the immunogenic glycosylated GPI precursors remain free at the parasite cell surface. *Int. J. Biochem. Cell Biol.* **38:** 1914–1925.

49. Bligh, E. G., and W. J. Dyer. 1959. A rapid method of total lipid extraction and purification. *Can. J. Biochem. Physiol.* **37:** 911–917.

50. Lowry, O. H., N. J. Rosebrough, A. L. Farr, and R. J. Randall. 1951. Protein measurement with the Folin phenol reagent. *J. Biol. Chem.* **193:** 265–275.

51. Carruthers, V. B., and J. C. Boothroyd. 2007. Pulling together: an integrated model of *Toxoplasma* cell invasion. *Curr. Opin. Microbiol.* **9:** 1–7.

52. Van der Zypen, E., and G. Piekarski. 1967. Endodyogeny in *Toxoplasma gondii*: a morphological analysis. *Z. Parasitenkd.* **29:** 15–35.

53. Baum, J., A. T. Papenfuss, B. Baum, T. P. Speed, and A. F. Cowman. 2006. Regulation of apicomplexan actin-based motility. *Nat. Rev. Microbiol.* **4:** 621–628.

54. Benning, C., and H. Ohta. 2005. Three enzyme systems for galactoglycerolipid biosynthesis are coordinately regulated in plants. *J. Biol. Chem.* **280:** 2397–2400.

55. Jouhet, J., E. Maréchal, and M. A. Block. 2007. Glycerolipid transfer for the building of membranes in plant cells. *Prog. Lipid Res.* **46:** 37–55.

56. Miège, C., E. Maréchal, M. Shimojima, K. Awai, M. A. Block, H. Ohta, K. I. Takamiya, R. Douce, and J. Joyard. 1999. Biochemical and topological properties of type A MGDG synthase, a spinach chloroplast envelope enzyme catalyzing the synthesis of both prokaryotic and eukaryotic MGDG. *Eur. J. Biochem.* **265:** 990–1001.

57. Awai, K., E. Maréchal, M. A. Block, D. Brun, T. Masuda, H. Shimada, K. I. Takamiya, H. Ohta, and J. Joyard. 2001. Two types of MGDG synthase genes, found widely in both 16:3 and 18:3 plants, differentially mediate galactolipid syntheses in photosynthetic and nonphotosynthetic tissues in *Arabidopsis thaliana. Proc. Natl. Acad. Sci. USA.* **98:** 10960–10965.

58. Maréchal, E., K. Awai, M. A. Block, D. Brun, T. Masuda, H. Shimada, K. I. Takamiya, H. Ohta, and J. Joyard. 2000. The multigenic family of monogalactosyldiacylglycerol synthases. *Biochem. Soc. Trans.* **28:** 731–738.

59. Awai, K., T. Kakimoto, C. Awai, T. Kaneko, Y. Nakamura, K. Takamiya, H. Wada, and H. Ohta. 2006. Comparative genomic analysis revealed a gene for monoglucosyldiacylglycerol synthase, an enzyme for photosynthetic membrane lipid synthesis in cyanobacteria. *Plant Physiol.* **141:** 1120–1127.

60. Andersson, M. X., M. H. Stridh, K. E. Larsson, C. Liljenberg, and A. S. Sandelius. 2003. Phosphate-deficient oat replaces a major portion of the plasma membrane phospholipids with the galactolipid digalactosyldiacylglycerol. *FEBS Lett.* **537:** 128–132.

61. Botté, C., C. Jeanneau, L. Snajdrova, O. Bastien, A. Imberty, C. Breton, and E. Maréchal. 2005. Molecular modelling and site directed mutagenesis of plant chloroplast MGDG synthase reveal critical residues for activity. *J. Biol. Chem.* **280:** 34691–34701.

62. Awai, K., H. Watanabe, C. Benning, and I. Nishida. 2007. Digalactosyldiacylglycerol is required for better photosynthetic growth of *Synechocystis* sp. PCC6803 under phosphate limitation. *Plant Cell Physiol.* **48:** 1517–1523.

63. Lebrun, M., V. B. Carruthers, and M. F. Cesbron-Delauw. 2007. *Toxoplasma* secretory proteins and their roles in cell invasion and intracellular survival. *In Toxoplasma gondii*: The Model Apicomplexan—Perspectives and Methods. K. Kim and L. M. Weiss, editors. Elsevier/North Holland, Amsterdam. 265–316.

64. Johnson, T. M., Z. Rajfur, K. Jacobson, and C. Beckers. 2007. Immobilization of the type XIV myosin complex in *Toxoplasma gondii. Mol. Biol. Cell.* **18:** 3039–3046.

65. White, M. W., M. E. Jerome, S. Vaishnava, M. Guerini, M. Behnke, and B. Striepen. 2005. Genetic rescue of a *Toxoplasma gondii* conditional cell cycle mutant. *Mol. Microbiol.* **55:** 1060–1071.

66. Wuhrer, M., C. Grimm, R. D. Dennis, M. A. Idris, and R. Geyer. 2004. The parasitic trematode *Fasciola hepatica* exhibits mammalian-type glycolipids as well as Gal(beta1-6)Gal-terminating glycolipids that account for cestode serological cross-reactivity. *Glycobiology.* **14:** 115–126.

67. Bottier, C., J. Gean, F. Artzner, B. Desbat, M. Pezolet, A. Renault, D. Marion, and V. Vie. 2007. Galactosyl headgroup interactions control the molecular packing of wheat lipids in Langmuir films and in hydrated liquid-crystalline mesophases. *Biochim. Biophys. Acta.* **1768:** 1526–1540.

68. Coutinho, P. M., E. Deleury, G. J. Davies, and B. Henrissat. 2003. An evolving hierarchical family classification for glycosyltransferases. *J. Mol. Biol.* **328:** 307–317.